VOL. 10, NO. 2, FEBRUARY 2015 ISSN 1819-6608
ARPN Journal of Engineering and Applied Sciences


www.arpnjournals.com

PRESSURE AND PRESSURE DERIVATIVE ANALYSIS FOR NATURALLY-FRACTURED FRACTAL RESERVOIRS

Freddy Humberto Escobar, Lorena Lopez-Morales and Karen Tatiana Gomez
Universidad Surcolombiana/CENIGAA, Avenida Pastrana, Neiva, Huila, Colombia
E-Mail: fescobar@usco.edu.co

ABSTRACT

Naturally fractured reservoirs have received considerable attention in the recent decades since more than half of the world oil reserves are found in this type of deposits; then, it is becoming fundamental a good characterization of these reservoirs and their understanding for having a better success in their exploitation and management. Generally, as originally proposed by Warren and Root, naturally-fractured formations are represented by a two scale model: a fracture network and a matrix. This modeling assumes that the fracture network is equivalent to a homogeneous medium fixed into a Euclidean geometry. However, it has been shown that the fracture networks are fractal elements which must be seen as alternative views for reservoirs with multiple scales and a network of non-Euclidean fractures. Fractal geometry is a good candidate for representing such systems. Several models and solutions based on the transient-pressure behavior have been presented in the literature with which were found that the change in pressure is a function of a power-law relationship where the exponent is related to the fractal dimension. In this work, direct expressions were developed from observing characteristic features on the pressure derivative log-log plot, so fracture permeability, fractal dimension conductivity index, flow capacity and storativity ratio can be estimated. The equations were successfully tested with synthetic examples.

Keywords: fractal dimension, conductivity index, interporosity flow parameter, storage coefficient, fractal reservoirs.

INTRODUCTION

The study and definition of the flow processes taking place in naturally-fractured formations is a big challenge since the fluid interaction modeling and the two forming sub-systems is a difficult milestone to achieve. Barenblatt and Zheltov (1960) were the first researchers who proposed radial flow in fractured formations. They took into account two porous media with different porosity and permeability.

Later, Warren and Root (1963) assumed the system as an ortogonal distributed fracture network. They presented an approximated solution and characterized the reservoir into two well-known parameters: the interpososity flow parameter, λ, and the dimensiónless storativity coefficient 9flow capacity), ω. Recognizing the need for further scope modeling, Abdassah and Ershaghi (1986) presented a model for triple-porosity systems which considers an additional medium additional to matrix and fractures. Escobar *et al.* (2004), Escobar, Rojas and Rojas (2014) and Escobar, Camacho and Rojas (2014) have used several triple-porosity models to develop practical methodologies for well test interpretation in such formations.

Throughout the time and collection of evidences researchers have found that fractures are fractal elements. In other words, they are geometrical objects which basic and irregular structured is repeated at different scales. These are characterized for having such properties as fractal dimension which provides a description of the space filled by a group of fractures. Reservoirs with such characteristics are named fractal reservoirs.

Chang and Yortsos (1990) proposed a model to describe the transient-pressure behavior in reservoir with different scales, poor fracture conductivity and irregular space distribution which is defined as a system constituted by a fractal fracture network embedded in a Euclidian matrix. For this, they proposed a modified version of the diffusivity equation for a single fluid flow in a fractal object for systems with only participation of the fracture network and systems with participation of both matrix and fracture network. They considered the location and distribution of the fracture network in the reservoir by introducing parameter Df which allows such characterization and also the conductivity given among the fracture network with the conductivity index, θ.

Camacho, Fuentes-Cruz and Vazquez (2008) also investigated the production-decline behavior in a naturally-fractured formations exhibiting single and double porosity with a fractal networks of fractures. They implemented previous versions of the fractal diffusivity equation with a more recent generalization of this equation to include a temporal fractional derivative.

Researchers on fractal reservoirs are very common. Among several we can name the works presented by Acuña, Ershaghi and Yortsos (1995), Beier (1994) and Olarewaju (1996)

Using the model proposed by Chang and Yortsos (1990), several expressions are presented in this paper based upon the behavior and characteristic features found in the pressure and pressure derivative versus time log-log plot by implementing the Direct Synthesis Technique (TDS), Tiab (1993), so the conductivity index, the fractal dimension, fracture bulk permeability and the Warren-and-Root parameters can be estimated. The expressions were proof using synthetic examples.

MATHEMATICAL BACKGROUND

The model proposed by Chang and Yortsos (1990) was used in this study to generate dimensionless

pressure and pressure derivative versus dimensionless time log-log plots considering the variation the fractal dimensión, *Df*, the conductivity index, θ, the flow capacity, λ, the storativity ratio, ω and bulk-fracture permeability, k_f.

The objective was the observation of the different patterns and features found on the pressure and pressure derivative curves (see Figure-1) so expressions were obtained from an adequate treatment of such behaviors. The complete detail of the original work was presented by Lopez-Morales and Gomez (2014). The dimensionless quantities taken into account by Chang and Yortsos (1990) are given below:

Dimensionless time:

$$t_D = \frac{0.0002637 t k_f}{c_f \mu r_w^{\theta+2} \phi_f} \quad (1)$$

Dimensionless pressure:

$$P_D = \frac{0.0445 h k_f (\Delta P)}{q B \mu r_w^{1-\beta}} \quad (2)$$

Dimensionless pressure derivative:

$$t_D * P_D{}' = \frac{0.0445 h k_f (t * P')}{q B \mu r_w^{1-\beta}} \quad (3)$$

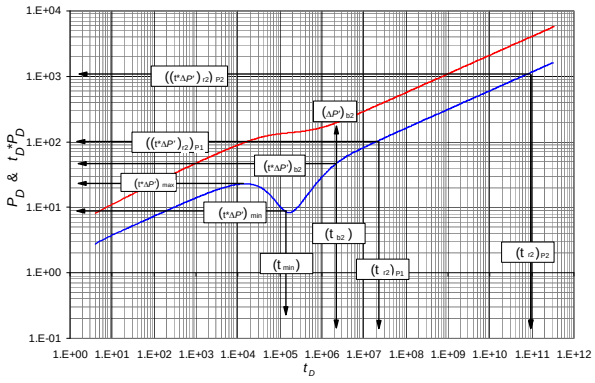

Figure-1. Characteristic points found on the pressure and pressure derivative plot in heterogeneous fractal reservoirs.

FRACTAL DIMENSION, *Df*

Figures-2 and 3 display the effect of the fractal dimension on pressure and pressure derivative for a fractal heterogeneous reservoir with constant values of θ =0.05, λ=1×10^{-9} and ω=1×10^{-3}.

Basically, it can be observed in Figura-2 that the fractal dimension, *Df,* alters the slope values during radial flow regime. The slope increases as the fractal dimension decreases; therefore, the maximum slope value is obtained for *Df*=1 and the lowest slope value is given for *Df*=2. It is also observed that this fractal parameter influences the curves to be shifted upwards as the fractal dimension decreases.

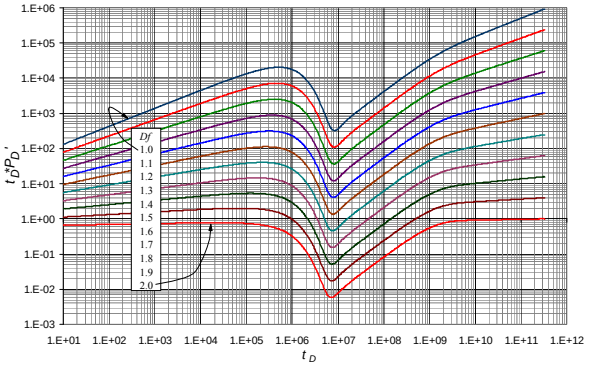

Figure-2. Influence of the fractal dimension on the derivative response.

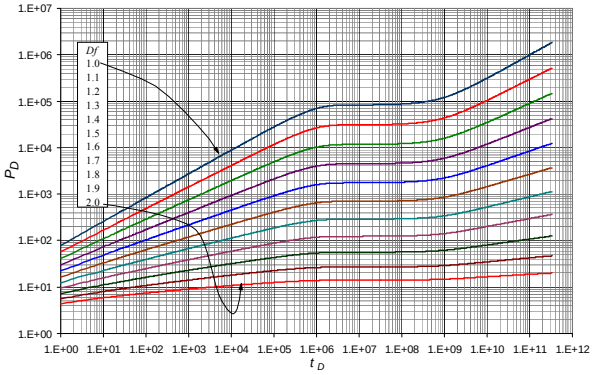

Figure-3. Influence of the fractal dimension on the pressure response.

Based upon these observations the following expression for the determination of the fractal dimension as a function of the pressure derivative slope during the second radial flow regime (after the trough) is given below:

$$Df = \frac{A + (C \times m) + \left(E \times (m)^2\right)}{1 + (B \times m) + \left(D \times (m)^2\right) + \left(F \times (m)^3\right)} \quad (4)$$

Where constants *A, B, C, D,* E and F are given for different sets as shown in Table-1.

It can be observed in Figure-3 that the pressure behavior follows the power-law condition which can be the main indicator that a fractal reservoir is dealt with. The clear slope change is observed and a flat region is presented in the middle of the two radial flow regimes which represent the transition between heterogeneous and homogeneous behavior.

The fractal dimension is proportional to the fracture index or fracture intensity of a given area. It means the greater the fractal dimension the greater the existing fractures in the studied zone.

Table-1. Coefficients for Equation (4).

Set number	1	2	3	4	5
θ	0.05	0.25	0.45	0.65	0.8
λ	1×10^{-9}	1×10^{-7}	1×10^{-6}	1×10^{-5}	1×10^{-4}
ω	1×10^{-3}	1×10^{-2}	5×10^{-2}	1×10^{-1}	3×10^{-1}
A	2.04942768	2.24975732	2.44983132	2.64993941	2.799850153
B	-3.33318545	-1.541209	-1.43189364	-1.34789006	-1.29644716
C	-8.79656412	-5.68356814	-5.93532474	-6.2192272	-6.42826815
D	0.13847047	0.02454796	0.0140922	0.00164203	0.001461292
E	6.74690488	3.43348909	3.48485751	3.56829279	3.626993927
F	-0.01223411	-0.00331232	-0.00254157	-0.00196032	-0.0031127

Selecting criteria

Since the correlation given by Equation 4 can be used with several set of constants (Table-1), it is necessary to establish which constant set is most appropriate. The pressure derivative slope of the second radial flow regime is used for this purpose. Refer to Table-2 to choose between two criteria:

Table-2. Criteria to select the *Df* Equation as a function of the slope.

Slope value	Applied criterion
$m < 0.29$	Least difference
$0.29 \leq m < 0.44$	Conjunto 3
$m \geq 0.44$	Least difference

Table-3. Least difference criterion for the calculation of *Df*.

Range	Limits			Set number		
	High	Medium	Low	Close medium	Close high	Close low
1	0.52	0.58	0.64	4, 5		5
2	0.37	0.455	0.54	4, 5	2	5
3	0.27	0.365	0.46	4, 3	1	4
4	0.17	0.28	0.39	2, 1	2	1
5	0.02	0.125	0.23	1	1	

Least difference criterion

Table-2 is used for the least difference criterion. Find there the value in which the slope value fits. Then, subtract the slope value from the limits given in Table-3 (low, medium and high). Find the smallest subtracted value (absolute value) in which the slope value falls and use the smallest difference. Once the least difference is chosen, refer to Table-3 and read from the right value the recommended equation number. Notice that two sets of constants are given in some boxes in the fifth column of Table-3. In such case is better to use the first number given from left to right. Use this number in Table-1 to choose your set of constants and use them in Equation 4 to determine *Df*.

Set 3

Constants numbered with 3 must be used for this criterion. Then, the constants are replaced into Equation 4 to find the value of the fractal dimension.

CONDUCTIVITY INDEX, θ

Figures 4 and 5 allow observing the conductivity index effect on the transient pressure behavior in a heterogeneous reservoir for Df=2, ω=0.3 and $\lambda=1\times10^{-4}$.

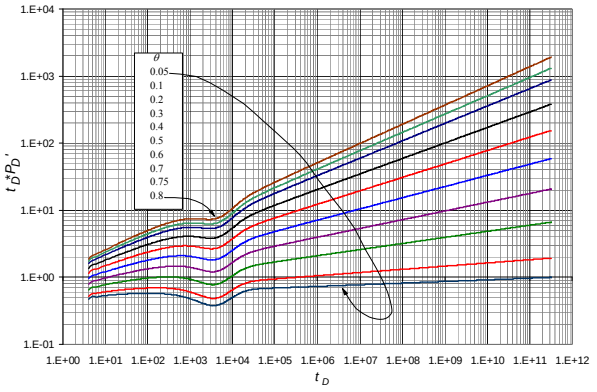

Figure-4. Influence of conductivity index, θ, on the pressure derivative response.

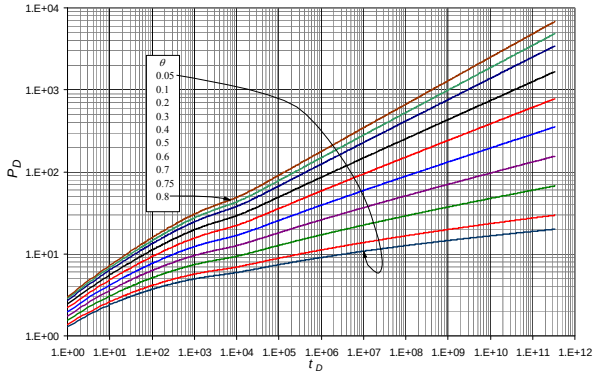

Figure-5. Influence of conductivity index, θ, on the pressure response.

From observation of Figure-4 it follows that as for the case of the fractal dimension the conductivity index also affects the radial-flow pressure derivative slope. The slope value increases as the conductivity index increases, with a maximum slope value when θ = 0.8 and lowest value of m when θ = 0.05. As θ decreases in value the pressure and pressure derivative curves are shifted upwards.

It can be seen in Figure-5 that the pressure derivative follows a power-law behavior. A clear pressure change is observed. The transition zone is hard to see since the ω value is too big.

$$\theta = \frac{A + (B \times Df) + (C \times m) + (D \times m^2)}{1 + (E \times Df) + (F \times m)} \quad (5)$$

Constants A, B, C, D and E given in Table-4 depend on the Df value estimated with Equation 4.

Chang and Yortsos (1990) also proposed an expression using the radial-flow pressure-derivative slope from which the conductivity index was solved fo

Table-4. Coefficients for equation (5).

	Application ranges				
	$1 \le Df < 1.3$	**$1.3 \le Df < 1.5$**	**$1.5 \le Df < 1.7$**	**$1.7 \le Df < 1.9$**	**$1.9 \le Df < 2$**
A	-2.26550513	-1.96948721	-1.73492605	-1.52575789	-1.15248778
B	1.18994348	1.02788916	0.89545061	0.77314003	0.580259
C	1.8343446	1.48917423	1.28362582	1.24781779	0.99201051
D	0.60219964	0.8765221	1.10187657	1.11562589	1.60822203
E	0.0148759	-0.06519897	-0.11927866	-0.14988095	-0.21859737
F	-0.89998567	-0.74649258	-0.58980289	-0.47481201	-0.14162367

Table-5. Coefficients for equation (8).

	Application ranges				
	$1 \le Df < 1.3$	$1.3 \le Df < 1.5$	$1.5 \le Df < 1.7$	$1.7 \le Df < 1.9$	$1.9 \le Df < 2$
A	1.482110404	0.955542559	0.838392191	0.703963482	0.406726714
B	-0.82859549	-0.63253775	-0.48565012	-0.3736336	-0.25851864
C	0.162089754	-0.34057856	-0.23702588	-0.18979038	-0.22748716
D	-0.96409836	-0.68836841	-0.50278852	-0.36858054	-0.26926113
E	-0.35837478	-0.64454501	-0.56378211	-0.52274181	-0.60824891
F	-0.70491282	-0.62924399	-0.53620842	-0.45732725	-0.31652

$$\theta = \frac{-Df}{m-1} - 2 \quad (6)$$

Where Df, the fractal dimension, and m is the radial-flow pressure-derivative slope.

BULK FRACTURE PERMEABILITY

The correlation for the estimation of the fracture permeability was obtained from the power-law behavior during the late radial flow regime (pressure derivative),

$$k_f = \mu \left[\frac{(0.0445h(t * \Delta P'))(c_f r_w^{\theta+2} \phi_f)^m}{(bqBr_w^{1-\beta})(0.0002637t)^m} \right]^{\frac{1}{m-1}} \quad (7)$$

Where ***b*** is defined by:

$$b = \frac{A + (B \times Df) + (C \times \theta) + (D \times \theta^2)}{1 + (E \times Df) + (F \times \theta)} \quad (8)$$

The set of constants for Equation 8 apply according the obtained *Df* value.

DIMENSIONLESS STORATIVITY RATIO, ω

The effect of the storativity coefficient on the pressure derivative and pressure is seen in Figures 6 and 7, respectively. These plots are given for values of *Df*=1.5, λ =1×10^{-6} and θ=0.45. Notice in Figure-6 that the minimum point given at the trough diminishes as the dimensionless storativity ratio increases until a point which is no longer seen. This corresponds to the homogeneous reservoir case. As far as the slope of the late radial flow regime is concerned no effect caused by the storativity ratio is seen since they converge into the same radial flow line. Then, the taken correlative criterion was the ratio between the trough and the maximum value of the pressure derivative just before the transition period starts. The following correlation was obtained:

$$\omega = \frac{A + \left(C \times \frac{(t_D * P_D')_{max}}{(t_D * P_D')_{min}}\right) + \left(E \times \left(\frac{(t_D * P_D')_{max}}{(t_D * P_D')_{min}}\right)^2\right)}{1 + \left(B \times \frac{(t_D * P_D')_{max}}{(t_D * P_D')_{min}}\right) + \left(D \times \left(\frac{(t_D * P_D')_{max}}{(t_D * P_D')_{min}}\right)^2\right) + \left(F \times \left(\frac{(t_D * P_D')_{max}}{(t_D * P_D')_{min}}\right)^3\right)} \quad (9)$$

Constants A, *B, C, D* and *E are* reported in Table-6.

It is observable in Figure-7 that when the storativity coefficient decreases, the pressure slope changes. They are better identified as a consequence of the typical transitions generated by the influence of different media affecting fluid flow in fractal naturally-fractured formations.

Table-6. Coefficients for Equation (9).

Universal application range	
A	-0.20610179
B	-1.45839236
C	-0.03408232
D	-0.55369927
E	0.000151803
F	0.002876531

FLOW CAPACITY PARAMETER, λ

Figures 8 and 9 illustrate the effect of the interporosity flow parameter on the transient behavior of a fractal natural-fractured reservoir under constant values of *Df*=1.3, θ=0.25 and ω=1×10^{-2}. Its effect is mainly reflected in the rapidity at which fluid transfers from matrix to fractures occurs.

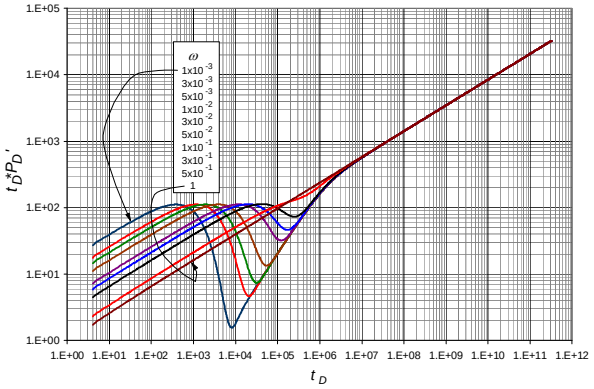

Figure-6. Effect of the dimensionless storativity ratio, ***ω***, on the dimensionless pressure behavior.

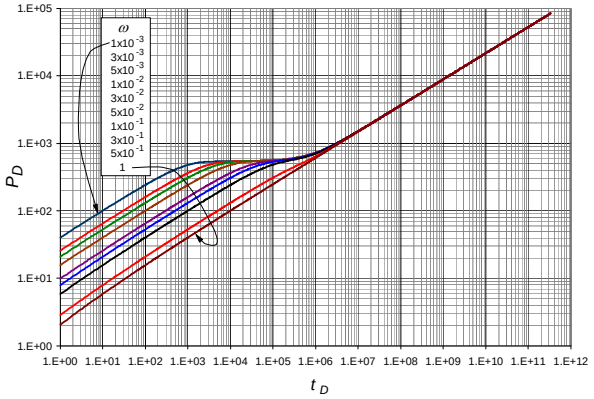

Figure-7. Effect of the dimensionless storativity ratio, ***ω***, on the dimensionless pressure derivative behavior.

As for the case of conventional naturally-fractured occurring formations, as seen in Figure-8, maximum and minimum points are affected by the value of λ. Also, the time at which the second radial flow regime shows up of is affected by the flow capacity value. In other words, the flow capacity affects the occurrence of the transition period.

In general terms, as the λ value decreases the appearance of the transition zone is delayed. The maximum and minimum pressure derivative values and their occurrence times also increase.

It can be seen in Figure-9 that as λ diminishes the better the identification of the transition zone. Besides, several variations in the transient behavior are observed as a consequence of the acting of the two different media on the fluid flow. Additionally, it was found that the start of second or late radial flow regime converges on the same set of points for different λ values. In other words, the length of the straight line of the radial flow regime changes but its location remains invariable (it does not shift along the time axis). Therefore, the used expression for the flow capacity estimation is not a function any time value on the radial flow regime. Then, an expression

presented by Tiab and Escobar (2003) based upon the time at the trough (minimum) is used here:

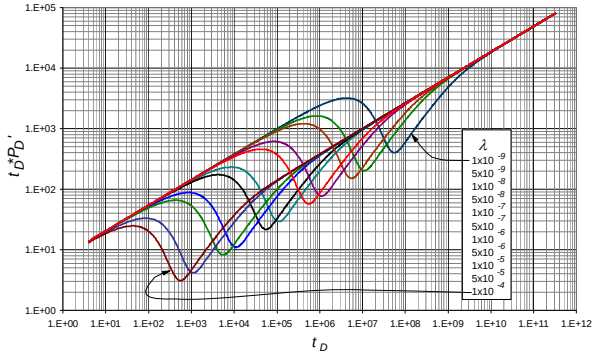

Figure-8. Flow capacity effect on pressure derivative response.

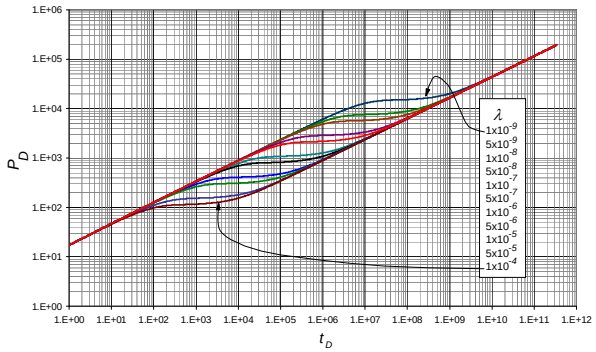

Figure-9. Flow capacity effect on the pressure response.

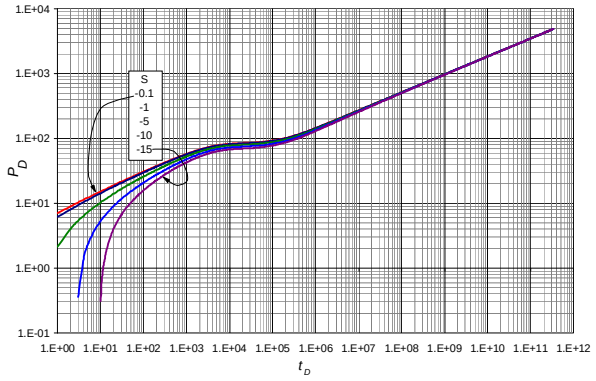

Figure-10. Effect of negative skin factor on the transient-pressure behavior of a fractal naturally-fractured reservoir.

$$\lambda = \frac{3792 \times (\phi c_t)_t \times \mu \times r_w^2}{k_f \times \Delta t_{\min}} \left[\omega \ln\left(\frac{1}{\omega}\right) \right] \tag{10}$$

SKIN FACTOR, *s*

The effect of positive skin factors in not seen in the simulated pressure behavior. Only negative skin factors have an influence on the pressure curve at very early times. This is because naturally-fractured formations are self-stimulated. Figure-10 is given for negative skin factors keeping constant the values of Df=1.7, θ=0.35. ω=2×10^{-2} and λ=4.6×10^{-6}.

For the estimation of the skin factor, an expression presented by Flamenco and Camacho (2001) is used. After some manipulations of that equation, it was obtained:

$$s = \left[\frac{\Delta P}{t * \Delta P'} - \frac{1}{\psi} \right] a \psi t^{\psi} \tag{11}$$

Where α and ψ are given by Equations 12 and 13, respectively:

$$\alpha = \frac{(2+\theta)^{2\psi-1}}{\psi\left[\Gamma(1-\psi)\right](1-\omega)^{\psi}} \tag{12}$$

$$\psi = \frac{1-\beta}{d - Df - \sigma + 2\theta + 2} \tag{13}$$

Table-7. Input parameters for examples.

	Example 1	Example 2
Parameter	**Value**	
q, BPD	250	370
C, bbl/psi	0	0
h, ft	160	60
c_{ma}, psi^{-1}	1x10^{-6}	2x10^{-6}
c_f, psi^{-1}	2x10^{-6}	1.5x10^{-6}
ϕ_{ma}, %	7	2
ϕ_f, %	30	17
B, rb/STB	1.1	1.23
μ, cp	1.2	1.35
r_w, ft	0.21	0.38
σ	0.1	0.1

EXAMPLES

In their original work, Lopez-Morales and Gómez (2014) tested the developed equations with 43 synthetic examples. Only two of them are presented here for practical purposes.

Synthetic Example 1

Pressure test was run in a heterogeneous fractal reservoir using as input data the information provided in the second column of Table-7. Pressure and pressure derivative versus time data are provided in Figure-11. It is required to characterize this test.

Solution: The below information was read from Figure-11;

$[(t^*\Delta P')_{r2}]_{P1}$ =	10 psi	$(t^*\Delta P')_{min}$=	0.07 psi
$(t_{r2})_{P1}$ =	200 hr	$(t^*\Delta P')_{max}$=	1.7 psi
$[(t^*\Delta P')_{r2}]_{P2}$ =	40	t_{b2} =	10 hr
$(t_{r2})_{P2}$ =	40000 hr	$(t^*\Delta P')_{b2}$=	4.5 psi
t_{min} =	0.047 hr	ΔP_{b2}=	19 psi

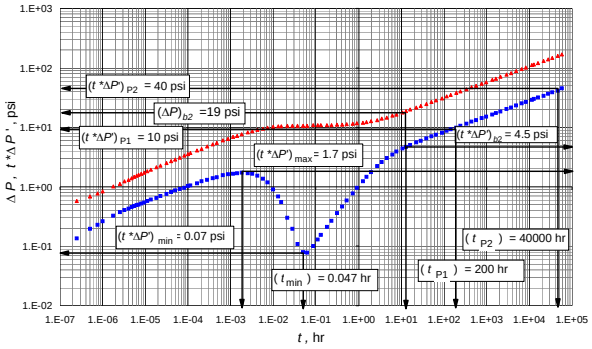

Figure-11. Pressure and pressure derivative vs. time log-log plot for example 1.

The first step was the estimation of the slope, m, of the late radial flow regime on the pressure derivative curve which resulted to be 0.2616 (the Reading points were 200, 10 and 40000, 40). Since this value is less than 29 then, from Table-2, we use the least difference criterion (second row). Looking at Table-3 we observe that the slope value better fits on range 4. Subtracting the slope (absolute value) from limits high, medium and low will give:

$$0.2616 - 0.17 = 0.0916$$
$$0.28 - 0.2616 = 0.0184$$
$$0.39 - 0.2616 = 0.1284$$

As observed in Table-3, the nearest value to the slope is the medium limit, then, the chosen set is 2. Correlation given by Equation 4 is used to estimate the Df value which resulted to be 1.6674. Since it fulfills the limiting condition $1.5 \leq Df < 1.7$, then, the set of constants given in Table-4 are used. The resulting value of θ was 0.262 estimated with equation (5). Using the same criterion as for the conductivity index, the fourth column of Table-5 is used to estimate a value of b which resulted to be 0.8442. This value is then replaced into correlation given by Equation (7) to provide the bulk fracture permeability, k_f, of 337.36 md. The minimum and maximum pressure derivatives are traduced into dimensionless quantities using Equation 3. ω and λ are estimated with correlations given by Equation (10) and (11), respectively. All, the main results are given in the third column of Table-8.

Table-8. Results for worked examples.

		Example 1	Example 2
Parameter	**Equation**	**Value**	
Df	4	1.6674	1.4242
θ	5	0.2620	0.8102
k_f, md	7	337.33 mD	148.9384
ω	9	2.9528×10^{-3}	9.523×10^{-2}
λ	10	2.4163×10^{-7}	2.640×10^{-8}
s	11	-2.5525	-10.7414

Synthetic Example 2

Similar to example 1, a simulated test was performed with the data given in the third column of Table-7 and the pressure and pressure derivative versus time data are shown in Figure-12. It is required for this test to estimate the permeability, fractal and naturally-fractured parameters.

Solution: The below information was read from Figure-12.

$[(t^*\Delta P')_{r2}]_{P1}$=	55000 psi	$(t^*\Delta P')_{min}$=	1646 psi
$(t_{r2})_{P1}$=	10000 hr	$(t^*\Delta P')_{max}$=	2630 hr
$[(t^*\Delta P')_{r2}]_{P2}$=	166000 psi	t_{b2} =	420 hr
$(t_{r2})_{P2}$	94700 hr	ΔP_{b2}=	25650 psi
t_{min}=	25 hr	$(t^*\Delta P')_{b2}$=	10900 psi

The procedure is the same as example 1 and results are reported in the fourth column of Table-8. For this case m = 0.4914 which is contained in range 2 of Table-3. The three differences are:

Low: $|0.37 - 0.4914| = 0.1214$

Medium: $|0.455 - 0.4914| = 0.0364$

High: $|0.54 - 0.4914| = 0.0486$

The medium difference suggests the use of constant set number 5.

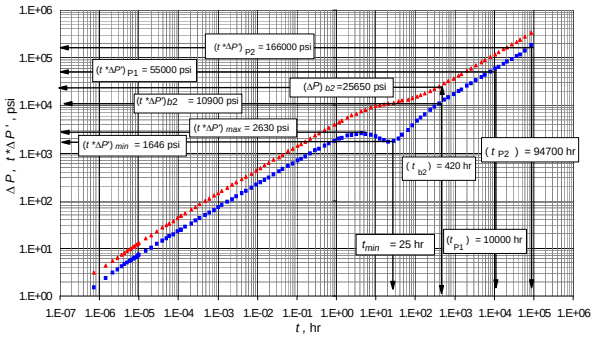

Figure-12. Pressure and pressure derivative vs. time log-log plot for example 2.

COMMENTS ON THE RESULTS

The results obtained from the proposed methodology agreed closely with those used for the simulations. However, it is important to take into account that the procedure outlined for the determination of the set of constants for the estimation of *Df* from the slope must be followed. The remaining estimations are strongly based upon the fractal dimension parameter. Then, the accuracy is a function of the above-mention selection.

The estimation of the conductivity index is very sensitive to the reading. Then, if possible use 5 decimal numbers.

5. CONCLUSIONS

a) Expressions for the determination of the fractal naturally-fractured reservoir parameters are introduced in this work and tested with synthetic examples.
b) The pressure response in fracture naturally-fractured reservoirs for the radial flow regime obeys the power-law relationship. This observation served as the starting point for the development of the developed expressions for reservoir characterization.
c) It was also verified that the complexity of the fracture network depends directly upon the size of the fractal dimension. This is then an indicator of the space amount used by the fracture network in a given area.
d) A dependency of the conductivity index on the fractal dimension was observed and used for the equation development.

However, a precise relationship between these two parameters is unknown.

REFERENCES

Abdassah. D. and Ershaghi. I. 1986. Triple-Porosity Systems for Representing Naturally Fractured Reservoirs." SPEFE (April) 113; Trans. AIME. 281.

Acuña J.A., Ershaghi I. and Yortsos Y.C. 1995. Practical Application of Fractal Pressure-Transient Analysis in Naturally Fractured Reservoirs. SPE Formation Evaluation. September. 173-179.

Barenblatt G.I., Zheltov. I.P., y Kochina. I.N. 1960. Basic Concepts in the Theory of Seepage of Homogenous Liquid in Fissured Rocks. PMM. Sovietic Applied Mathematics and Mechanics. pp.24-25.

Beier. R.A. 1994. Pressure-Transient Model for a Vertically Fractured Well in a Fractal Reservoir. SPE Formation Evaluation. June 122.

Camacho. R. Fuentes-Cruz. G. and Vasquez. M. A. 2008. Decline-Curve Analysis of Fractured Reservoirs With Fractal Geometry. Society of Petroleum Engineers. doi:10.2118/104009-PA. June 1.

Chang J. and Yortsos. Y.C. 1990. Pressure Transient Analysis of Fractal Reservoirs. SPE Formation Evaluation. 289. March. 31.

Escobar. F. H., Saavedra. N. F.. Escorcia. G. D. and Polania. J. H. 2004. Pressure and Pressure Derivative Analysis without Type-Curve Matching for Triple Porosity Reservoirs. Society of Petroleum Engineers. doi:10.2118/88556-MS. January 1.

Escobar. F.H., Rojas. J.D. and Rojas. R.F. 2014. Pressure and Pressure Derivative Analysis for Triple-Porosity and Single-Permeability Systems in Naturally Fractured Vuggy Reservoirs. Journal of Engineering and Applied Sciences. 9(8): 1323-1335.

Escobar. F.H., Camacho. R.G. and Rojas. J.D. 2014. Pressure and Pressure Derivative Analysis for Triple-Porosity and Dual-Permeability Systems in Naturally Fractured Vuggy Reservoirs. Paper sent to Journal of Engineering and Applied to request publication.

Lopez-Morales L. and Gomez, K.T. 2014. Análisis de Presión y Derivada de Presión en Yacimientos Heterogéneos Fractales. B.Sc. Thesis. Universidad Surcolombiana. Neiva (Huila), Colombia.

Olarewaju J.S. 1996. Modeling Fractured Reservoirs with Stochastic Fractals. Paper SPE 36207 presented at the 7th Abu Dhabi International Petroleum Exhibition and Conference held in Abu Dhabi. 13-16, October.

Tiab. D. 1993. Analysis of Pressure and Pressure Derivative without Type-Curve Matching: 1- Skin and Wellbore Storage. Journal of Petroleum Science and Engineering. 12: 171-181.

Tiab D. and Escobar F.H. 2003. Determinación del Parámetro de Flujo Interporoso a Partir de un Gráfico Semilogarítmico. X Congreso Colombiano del petróleo (Colombian Petroleum Symposium). October. 14-17. ISBN 958-33-8394-5. Bogotá (Colombia).

Warren. J.E. y Root. P.J. 1963. The Behavior of Naturally Fractured Reservoirs. SPEJ. pp. 245-255. September.

Nomenclature

B	Volume factor , rb/STB
C	Welbore storage coefficient, bbl/psi
c_f	Fracture network compressibility, 1/psi
c_{ma}	Matrix compressibility, 1/psi
c_t	Total compressibility, 1/psi
d	Euclidian dimension
h	Formation thickness, ft
k_f	Fracture network permeability, md
m	Pressure derivative slope of late radial flow regime
P	Pressure, psi
P_D	Dimensionless pressure
q	Flow rate, BPD
r_w	Well radius. ft
s	Skin factor
t	Time, hr
t_D	Dimensionless time
t_D*P_D'	Dimensionless pressure derivative
$t*\Delta P$'	Pressure derivativ,. psi

Greek

α	Variable defined by Equation (12)
β	Df-θ-1
Δ	Change, drop
σ	Matrix- fractures interaction index
ψ	Variable defined by Equation (13)
ϕ_f	Fracture porosity
ϕ_{ma}	Matrix porosity
ϕ_t	Total porosity
Γ	Gamma function
λ	Interporosity flow parameter
θ	Conductivity index
μ	Viscosity, cp
ω	Dimensionless storativity ratio

Suffixes

b_2	Start of second radial flow regime
D	Dimensionless
min	Minimum
max	Maximum
f	Fracture
ma	Matrix
$r2$	Late radial
$P1$	Initial point
$P2$	Final point